Journal of Sustainable Mining 16 (2017) 47–54

HOSTED BY

Contents lists available at ScienceDirect

Journal of Sustainable Mining

journal homepage: http://www.elsevier.com/locate/jsm

Research paper

Experimental study on fracturing coal seams using CaO demolition materials to improve permeability

Yibo Tang [a, b, *], Liang Yuan [a], Junhua Xue [a], Changrui Duan [a]

[a] State Key Laboratory of Deep Coal Mining and Environment Protection, Huainan 232000, China
[b] College of Mining Technology, Taiyuan University of Technology, Taiyuan 030024, China

ARTICLE INFO

Article history:
Received 10 May 2017
Received in revised form
9 July 2017
Accepted 31 July 2017
Available online 2 August 2017

Keywords:
Soundless chemical demolition
Coal seam
Gas drainage
CaO

ABSTRACT

Currently, methane gas disasters in underground coal mines are a major problem which seriously threatens safe mining. This study employed soundless chemical demolition for fracturing coal seams with low permeability. Additionally, the fracturing theory and failure mechanisms of soundless chemical demolition agents were investigated. Materials such as CaO, naphthalene-based water reducer, sodium gluconate and silicate cement were used to prepare the novel soundless chemical demolition agent, whose optimum proportion was discovered to be 90:3:5:7 by carrying out orthogonal experiments. The innovative demolition agent cracked briquettes and the maximum width of cracks reached 16.33 mm, showing significant potential for improving the permeability of coal seams.

1. Introduction

Gas disasters are one of the primary hazards of coal mines in China, causing severe casualties and property losses (Xue & Yuan, 2017; Yuan, 2016). The high concentration of gas in a coal mine roadway will lead to gas combustion (Jiang, Lin, Shi, Zhu, & Li, 2011) and explosion (Gao, Fu, & Nieto, 2016; Lin et al., 2013), while high gas content in coal seams generally causes dynamic disasters like coal and gas outbursts (An, Cheng, Wang, & Li, 2013; Aguado & Nicieza, 2007). Therefore, reducing gas content in coal seams is the key to controlling gas disaster in mines (Karacan, Ruiz, Cotè, & Phipps, 2011; Tang, 2015). Nowadays, approaches to gas control mainly depend on gas extraction, but due to the low permeability coal seams in China, extracting gas from boreholes has low efficiency and fails to promote gas utilization and reduce gas disaster in mines (Xue et al., 2016). To solve this problem, improving the permeability of coal seams is a top priority (Toraño, Torno, Alvarez, & Riesgo, 2012; Wang et al., 2013). With this in mind, Yuan (2011) proposed a theory of coal and gas to remarkably increase the efficiency of gas extraction by exploiting protective coal seams to extract and release gas pressure. However, this method has a limited application scope and is not applicable to mines that do not have certain conditions. An et al. (2015) tried to utilize a numerical model to determine the permeability changes of coal seams after injecting CO_2, so as to research the impacts of CO_2 injection on coal-bed methane recovery. To achieve permeability improvement and pressure relief in local coal seams, some scholars suggested using hydraulic measures to increase the permeability of coal seams. For example, Germanovich, Astakhov, Mayerhofer, Shlyapobersky, and Ring (1997) surveyed hydraulic fracturing in several fields and built corresponding models. A series of hydraulic cutting approaches were proposed by Lin et al. (2015) which exert significant effects on improving the efficiency of gas extraction by drilling boreholes, while Song et al. (2015) evaluated the effects of hydraulic fracturing for coal seams using a direct current method. Generally speaking, these methods are complex, involve high costs and are still in the exploration stage at present. Blasting is another choice to increase the permeability of coal seams, as high-energy shock waves generated by blasting can destroy coal near boreholes, leading to the fracture of coal seams and stress reduction, and thus increasing the channels for gas migration (Zhu, Gai, Wei, & Li, 2016). However, a huge amount of potential risks are likely to occur, such as inducing coal and gas outbursts, and igniting gas. In contrast, soundless chemical demolition technology is a potential method for fracturing coal seams that can be applied to augment the low permeability of coal seams (Fukui & Nagaishi, 2001; Gambatese, 2003; Natanzi & Laefer, 2015). If there is excessive free calcium oxide (*f*-CaO) in concrete, lime calcined at high temperature will

* Corresponding author. 79 Yingze West Avenue, Taiyuan, Shanxi Province, China.
E-mail address: tangyibo11@126.com (Y. Tang).

http://dx.doi.org/10.1016/j.jsm.2017.07.002

gradually form calcium hydroxide [$Ca(OH)_2$] through hydration, resulting in the spalling of concrete. Hinze and Nelson (1996) studied a soundless breaking agent, and they found that the primary principles of this in chemical demolition depend on the volume expansion of $Ca(OH)_2$ generated in the chemical reactions of CaO and water. In underground collieries, when compared with their original state, the permeability of a coal seam will increase remarkably when it has been fractured. Obviously, it can be regarded as a potentially effective method that fractures coal seams using CaO demolition materials to improve permeability. Therefore, this study employed a soundless chemical demolition agent for creating cracks in coal seams and thus augmenting the permeability of coal seams.

2. Material and methods

2.1. Experimental material

This experiment adopted briquettes as the object; the raw materials for producing briquettes included pulverized coal, gypsum, concretes and water. The coal specimens were obtained from coal seams in the #3 Sihe Coalfield, Jincheng, Shanxi province, China, with diameters ranging from 1.0 to 3.0 mm. The technical parameters of the coal sample are shown in Table 1. GRG gypsum powder (obtained from CAO CHANG PLASTER CHEMICAL Co., Ltd.) was selected for the test, and had normal consistency, flexural strength, expansion coefficient, an initial setting time and final setting time of 30%, 8 MPa, 0.08%, 10–12 min and 30 min, respectively. Silicate cement (obtained from AHHUI CONCH CEMENT Co., Ltd.) was used and its cement fineness and strength grade were 30% and 32.5 and its initial setting time and final setting time were 2 h and 3 h, respectively. The preparation of briquettes was as follows: the proportion of pulverized coal (1000 g), gypsum powder (500 g) and concretes (500 g) was 2:1:1, together with 1000 mL water measured by a measuring cylinder. These materials were stirred sufficiently before pouring the resulting slurry into a 15 cm × 15 cm × 10 cm (length × width × height) mould (Fig. 1); afterwards, a 20-cm-long PVC pipe with a hole diameter of 20 mm was fixed in the center of the mould. After being cured for a week in the mould, a blast-hole of 20 mm in diameter and 9 cm deep was arranged in the center of the briquettes taken out of the mould.

2.2. Orthogonal experiment

On the basis of determining the components of the chemical demolition agent, an orthogonal experiment was conducted to decide the proportions of each component. The prepared chemical demolition agent mainly consisted of quicklime (Ca content≥90.0%, Particle size: 0.150 mm–0.180 mm), a naphthalene-based water reducer (obtained from SHANGHAI LIRUI CHEMICAL Co. Ltd.), sodium gluconateretarder (obtained from TIANJIN DINGSHENGXING CHEMICAL Co. Ltd.) and silicate cement (obtained from AHHUI CONCH CEMENT Co., Ltd.). In order to ensure the accuracy of the experiment, the size of the briquettes were unified. Thus, the optimal proportion can be acquired by conducting experiments with chemical demolition agents with different proportions. Various levels of components selected in the orthogonal experiment are shown in Table 2: 70, 80 and 90 portions of quicklime, 1, 3 and 5 portions of naphthalene-based water reducer, 1, 3 and 5 portions of sodium gluconate, and 3, 5 and 7 portions of silicate cement were adopted. The proportion of water remained the same. The chemical demolition agents were prepared according to the aforementioned portions, and then filled in to the blast-hole of the briquettes after being mixed with water to a sufficient degree. After setting the fracturing agents for 4, 8, 16 and 24 h, the maximum widths of primary cracks were recorded to evaluate the fracturing effects.

Table 1
Technical parameters of coal sample.

Name	Mad%	Ad%	Vad%	Fcd%	Coal rank
Sihe Coal	2.15	9.34	5.12	83.39	anthracite

a) Mould

b) briquette coal

Fig. 1. Mould and finished product of briquette coal.

3. Discussion

3.1. Fracturing effects

Compared with other fracturing methods, the approach of CaO demolition is a slow developing process. After the demolition agent

Table 2
Orthogonal test result of static fracturing experiment.

No.	Calcium oxide/ portion	Naphthalene superplasticizer/ portion	Sodium gluconate/ portion	Portland cement/ portion	Average width of crack/ mm	Maximum width of crack/ mm
1	70	1	1	3	0	0
2	70	3	3	5	0	0
3	70	5	5	7	0	0
4	80	1	3	7	7.2	13.6
5	80	3	5	3	8.18	15.0
6	80	5	1	5	0	0
7	90	1	5	5	4.7	12.0
8	90	3	1	7	9.28	16.3
9	90	5	3	3	5.4	12.1

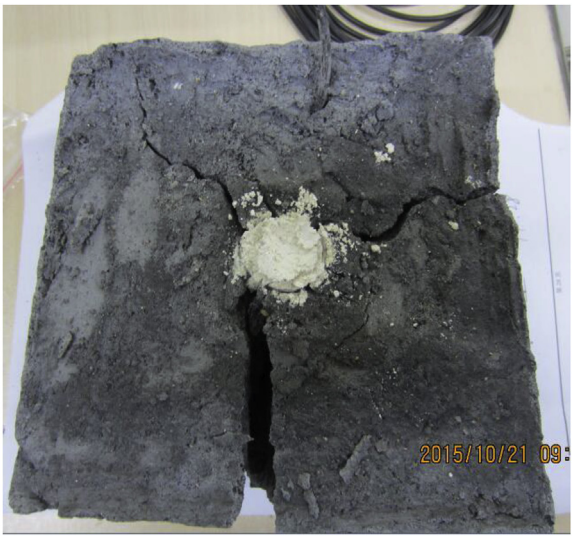

a)Top view

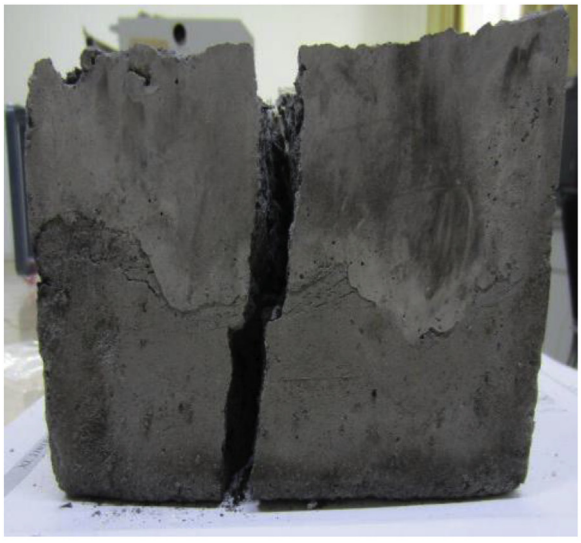

b) Side view

Fig. 2. Fracturing effect of specimen (briquette).

is utilized, the briquette coal is successfully fractured within hours (Fig. 2). According to the orthogonal experiment, results showed that no cracks were generated in the briquettes loaded with 70 portions of quicklime in groups 1, 2 and 3. The maximum widths of primary cracks in group 4 at 4, 8, 16, 24 h were 0, 3.8, 11.4 and 13.6 mm, respectively, with an average width of 7.2 mm. Group 5 presented the maximum widths of primary cracks of 0, 4.7, 13.0 and 15.0 mm while the average width was 8.18 mm. By comparison, no cracks were found in group 6. It can be found that the maximum widths of primary cracks in group 7 were 0, 2.4, 4.4 and 12.0 mm respectively, and 4.7 mm on average. The maximum widths of primary cracks in group 8 were 0, 6.2, 14.6, and 16.3 mm with an average width of 9.28 mm, while those in group 9 were 0, 0, 9.5 and 12.1 mm with an average width of 5.4 mm. As part of this research intuitive analysis was carried out on the results of the orthogonal experiment (Table 2), which analyzed the experimental effects of the 4 factors under levels I, II and III, calculated averages and ranges of each level, and discussed the variances. Changes in the fracturing effects of chemical demolition agents with varying factors and levels are shown in Tables 3 and 4. Preliminary analysis of the data, allowed for the optimum proportion of the chemical demolition agent to be obtained, which was: 90 portions of quicklime, 3 portions of naphthalene-based water reducer, 5 portions of sodium gluconateretarder and 7 portions of silicate cement. In other words, the optimum ratio of quicklime, naphthalene-based water reducer, sodium gluconateretarder and silicate cement concrete is 90:3:5:7. Obviously, the contents of quicklime exerted an important influence on fracturing effects, which was increasingly apparent as the content increased. At the same time, the content of other components also affected the fracturing effect. With the increase of the water reducer, the fracturing effect is weakened remarkably. In contrast, when the retarder is increased, the demolition effect is enhanced.

3.2. XRD tests

This study employed the optimum ratio of the agent with optimal fracturing effects selected through the orthogonal experiment and conducted X-ray diffraction analysis. Then, the microstructure and component changes of the chemical demolition agent were analyzed. The chemical demolition agent with the optimum ratio was used to test 4 groups of specimens. The specimens were treated as follows: group 1 used the chemical demolition agent without water; groups 2, 3 and 4 used the chemical demolition agents at 5, 10 and 15 h after the addition of water, respectively. By detecting component changes of fracturing agents at different time points before and after water being added, this study indirectly analyzed the expansion process of the chemical demolition agent. The results of different groups are illustrated in Fig. 3. It can be seen that $Ca(OH)_2$ was not detected in group 1 from the phase analysis of specimens without water. When compared with the spectrum of

Table 3
Range analysis of the orthogonal test.

Indicator	CaO	Naphthalene superplasticizer	Sodium gluconate	Silicate cement
I	0	11.90	9.28	13.58
II	15.38	17.46	12.60	4.70
III	19.38	5.40	12.88	16.48
K_1=I/3	0	3.97	3.09	4.53
K_2=II/3	5.13	5.82	4.20	1.57
K_3=III/3	6.46	1.80	4.29	5.49
Range	6.46	4.02	1.20	3.93

Table 4
Variance analysis of the orthogonal test.

Indicator	Sum of squares of deviations	Degree of freedom	variance ratio	Critical value of variance ratio
CaO	69.79	2	26.11	19.00
Naphthalene superplasticizer	24.29	2	9.09	
Sodium gluconate	2.67	2	1.00	
Silicate cement	25.12	2	9.40	
Errors	2.67			

group 1, remarkable variations took place in the spectrum of group 2, after adding water for 5 h a phase peak corresponding to $Ca(OH)_2$ occurred in Fig. 3b. The spectrum of group 4 (15 h after the addition of water) showed that the phase peak corresponding to CaO disappeared. By comparing the spectra of the 4 groups at different time points, it was found that variations between Fig. 3a and b were more obvious than those among Fig. 3b, c and d. Therefore, the major substance variation in the chemical demolition agent was the transformation of CaO to $Ca(OH)_2$, accompanied with the volume expansion of the fracturing agent. Under confined conditions, the expansion produced expand pressure against the hole walls, which finally resulted in the cracking of briquettes. It can be illustrated that the generation rate of $Ca(OH)_2$ in the reaction of CaO and water in 0–5 h was higher than that in 5–10 h and 10 h–15 h. Considering that the main reason for briquette cracking was the process of the formation of $Ca(OH)_2$, it can be implied that the growth speed of expand pressure varied before the pressure of the chemical demolition agent reached the maximum. In the atlas of the agent at 15 h after the addition of water, no CaO appeared so it can be inferred that the expand pressure of the chemical demolition agent was completely released in 10–15 h. In the initial period after setting the agent, the hydration degree of the chemical demolition agent was limited and clearances existed among agent particles, so limited expansion pressure was generated. As CaO fully reacted with water, the chemical demolition agent expanded until the clearances of particles were filled, so great pressure was exerted by the chemical demolition agent against the hole walls which led to the briquette cracking and thus provided a greater gas-flow channel in coal seams. This phenomenon indicates that the chemical demolition technology depends on the hydration of calcium-based materials and pressure produced by the expansion of molecular lattices at a microscopic level. Macroscopically, the chemical demolition agent releases pressure on to the hole walls, resulting in coal failure.

3.3. Mechanism of chemical demolition

For single holes, the diameter of boreholes is far smaller than the size of surrounding rocks and borehole depth and the properties in each direction were the same when chemical demolition agents were expanded. Moreover, circular blasting holes are symmetrical. For these reasons, the stresses on the internal walls of blasting holes were spatially axisymmetrical, therefore the stresses on internal hole walls were symmetrical with respect to the z axis. Therefore, a simplified cylinder model with thick walls was used for this research.

Before cracks appeared in the surroundings of the boreholes, units a, b, c and d at the edge of boreholes were studied, as shown in Fig. 4. Because the shapes changed symmetrically about the axis of the borehole, the displacement u of each point along the direction of the radius is only related to radius ρ rather than angle φ. The side ad of the unit moves to $a'd'$ after shape change, so the hoop and radial strains are obtained (Formula (1)).

$$\begin{aligned}\varepsilon_\varphi &= \frac{a\prime d\prime - ad}{ad} = \frac{(\rho+u)d\varphi - \rho d\varphi}{\rho d\varphi} = \frac{u}{\rho}\\ \varepsilon_\rho &= \frac{a\prime d\prime - ab}{ab} = \frac{[d\rho + (u+du) - u] - dp}{d\rho} = \frac{du}{d\rho}\end{aligned} \tag{1}$$

where, ε_φ and ε_ρ are the hoop strain and radial strain, respectively.

According to Fig. 4, the static equilibrium equation is (Formula (2)):

$$\frac{d\sigma_\varphi}{d\rho} + \frac{\sigma_\rho - \sigma_\varphi}{\rho} = 0 \tag{2}$$

where, σ_ρ and σ_φ are the radial and hoop stresses separately.

Under the conditions of linear elasticity, the relationship between stress and strain is obtained according to Hooke laws (Formula (3)), thus solving radial stress σ_ρ and hoop stress σ_φ.

$$\left.\begin{aligned}\sigma_\rho &= \frac{p_1 a^2}{b^2 - a^2}\left(1 - \frac{b^2}{\rho^2}\right)\\ \sigma_\varphi &= \frac{p_1 a^2}{b^2 - a^2}\left(1 + \frac{b^2}{\rho^2}\right)\end{aligned}\right\} \tag{3}$$

where, p_1 is expand pressure at $\rho =$ a. a, b and ρ are the inner and outer diameters of the unit as well as the distance of the unit away from the original point, respectively.

In accordance with (Formula (3)), σ_ρ and σ_φ represent constant compressive stress and tensile stress on hole walls and they reach the maximum at $\rho = a = R$ at the lateral side of borehole walls.

From the viewpoint of the chemical reaction, the reaction equation (Formula (4)) of CaO and water is expressed as follows:

$$CaO + H_2O \rightarrow Ca(OH)_2 \tag{4}$$

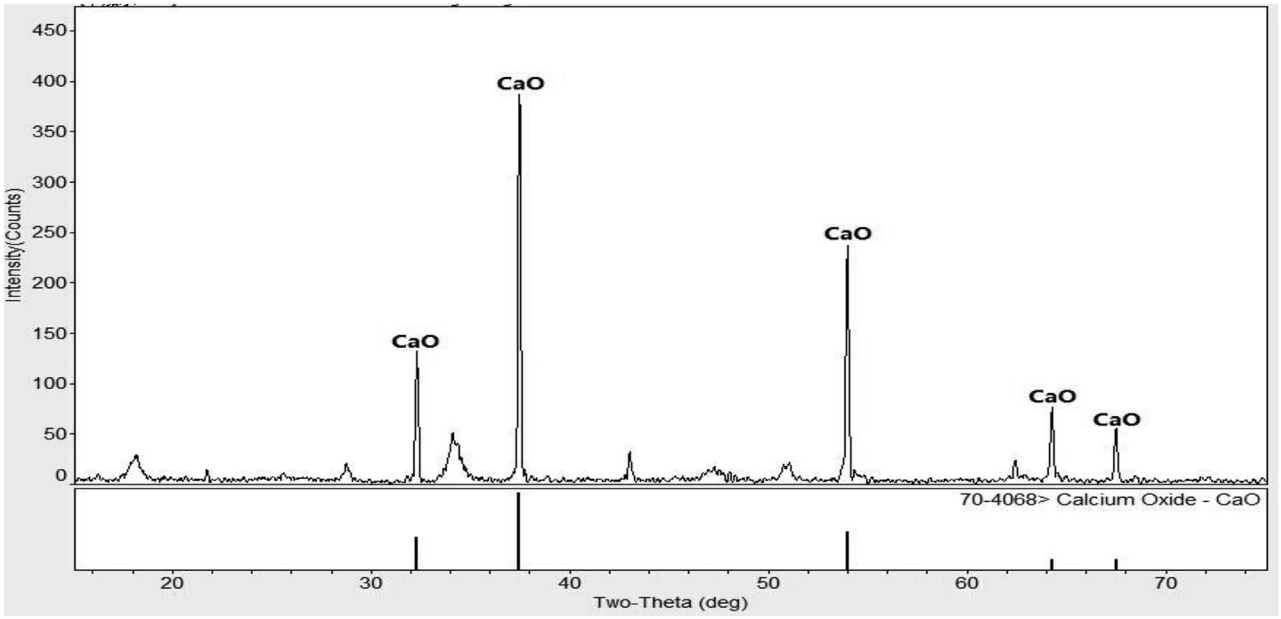

a) Dried sample

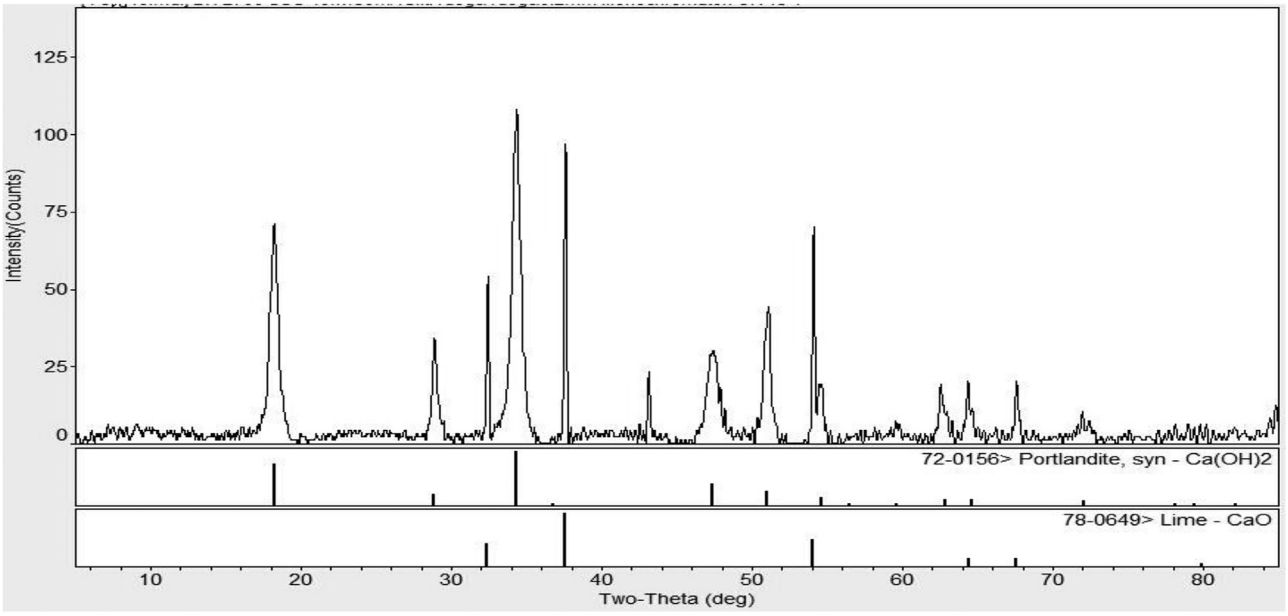

b) Sample after adding water by 5h

Fig. 3. XRD analysis result.

$Ca(OH)_2$ crystallization has a layered structure, of which the internal structure is hexagonal and closed-packed, and layers are connected with weak chemical bonds. According to the theory of quicklime hardening, the hardening process of quicklime can be divided into dissolution, gelation, coagulation, crystallization, drying and carbonization. When quicklime is mixed with water, the surface of CaO particles are hydrated immediately to form $Ca(OH)_2$. After the forming of a saturated solution by being dissolved in water, $Ca(OH)_2$ stops dissolving and is precipitated in the form of colloids; this is accompanied with a great amount of heat release. Due to water being absorbed inside quicklime particles, colloidal particles are tightly bonded, resulting in condensation. Due to the thermodynamic stability of the dispersion system of colloids, the finest part of colloid dissolves, while coarse particles enlarge after absorbing solutes. This recrystallization is the main reason for the strength increase of slurry, and this strength is called crystallization

strength. Afterwards, as water vaporizes and the slurry dries, $Ca(OH)_2$ solution is over saturated, which also aids its crystallization and hardening. Moreover, $Ca(OH)_2$ is transformed into $CaCO_3$ by absorbing CO_2 in the air, leading to the augmentation of solid volume, which further compacts and strengthens the hardening quicklime. The specific surface area of $Ca(OH)_2$ formed in the reaction of quicklime without enough water is extremely large and loose. The apparent density needs to be selected for calculation while analyzing the volume changes of the chemical demolition agents before and after reactions, because molar volume measures the volume of compacted molecules. The molecular weight of CaO is 56.08 g and the apparent density is 3.35 g/cm^3 so its molar volume is 16.74 cm^3, while those of $Ca(OH)_2$ are 74.08 g, 2.24 g/cm^3 and 33.07 cm^3 respectively. As a result, the increment of solid volume of CaO is 98% according to (Formula (5)).

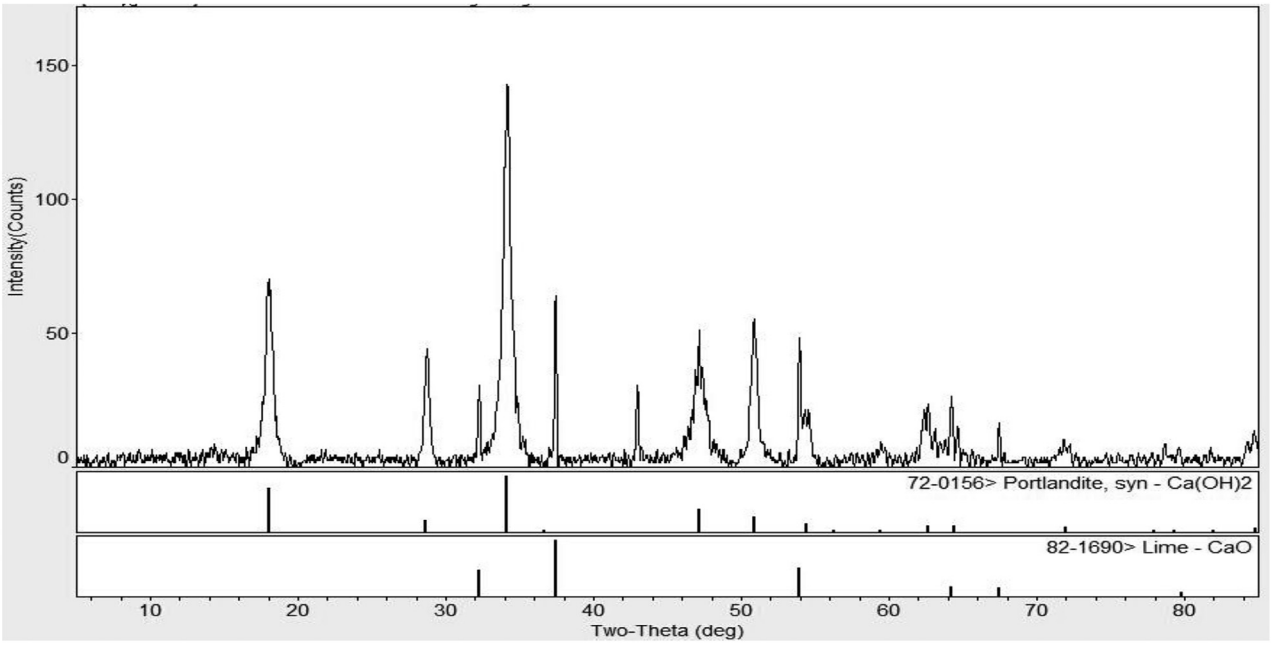

c) Sample after adding water by 10h

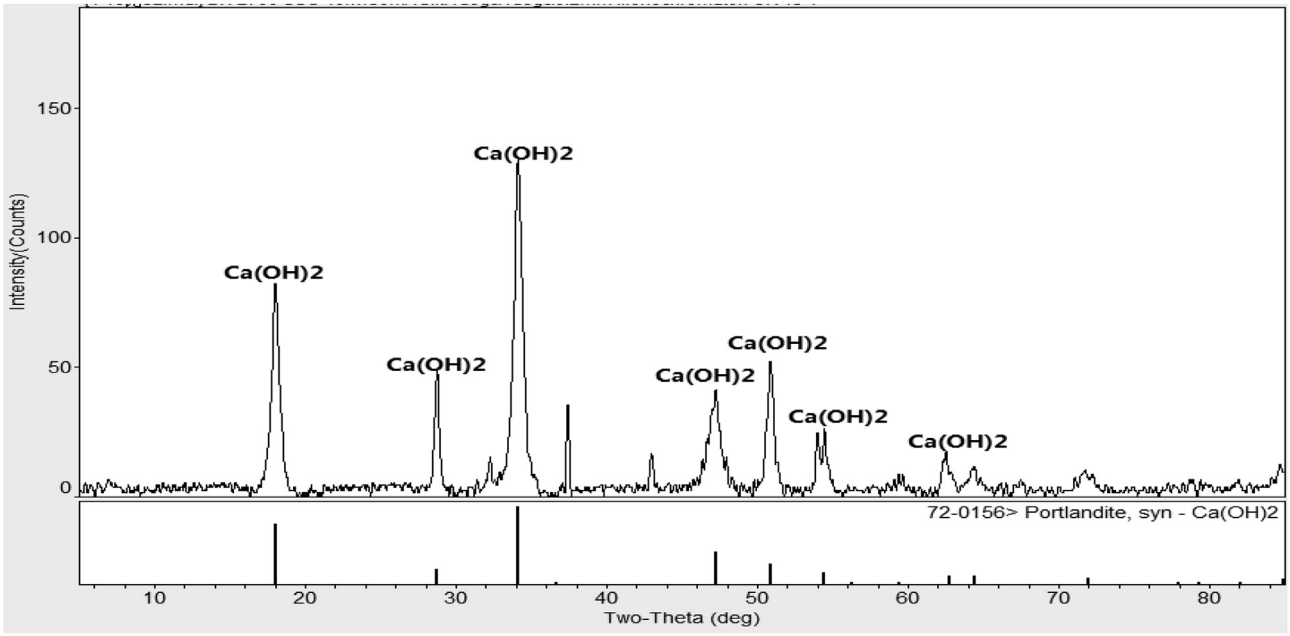

d) Sample after adding water by 15h

Fig. 3. (*continued*).

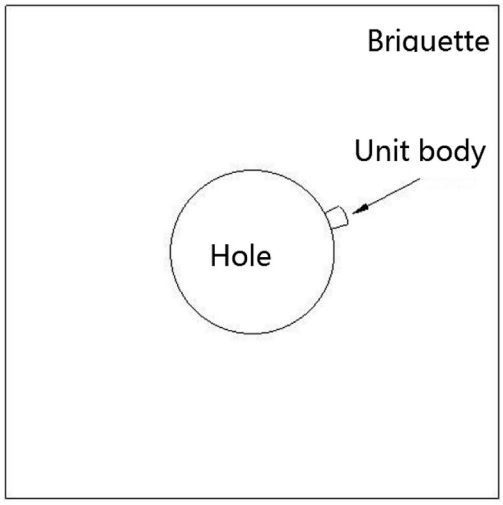

a) Model of coal briquette

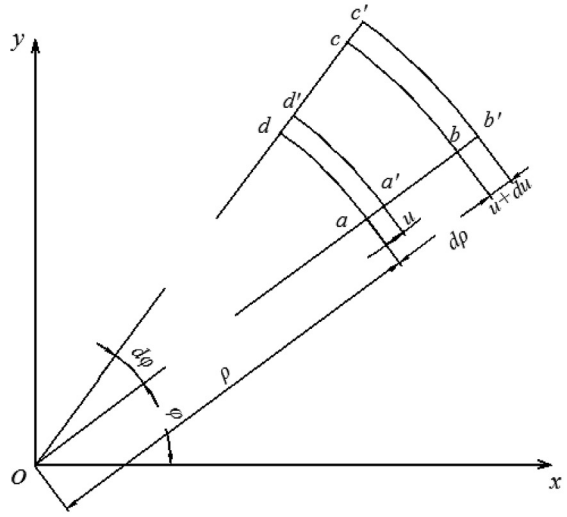

b) Strain of the unit

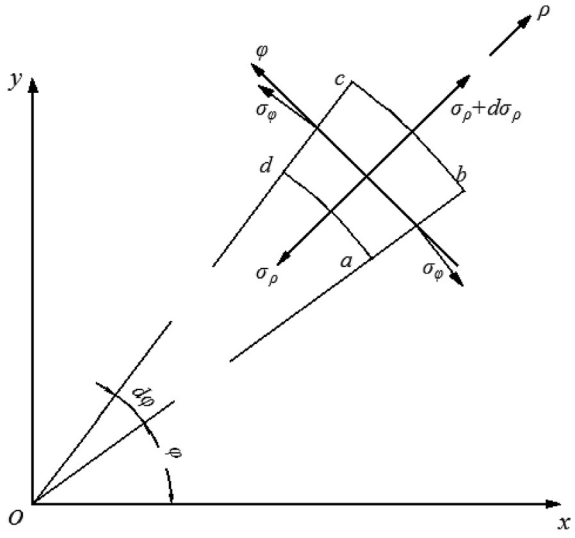

c) Force analysis of the unit

Fig. 4. Theoretical analysis of static fracturing of briquette.

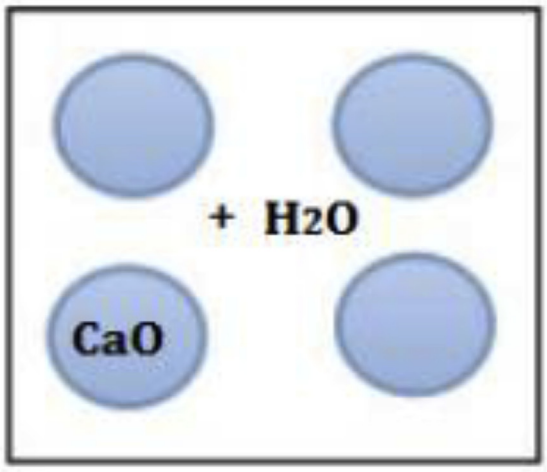

a) Original state

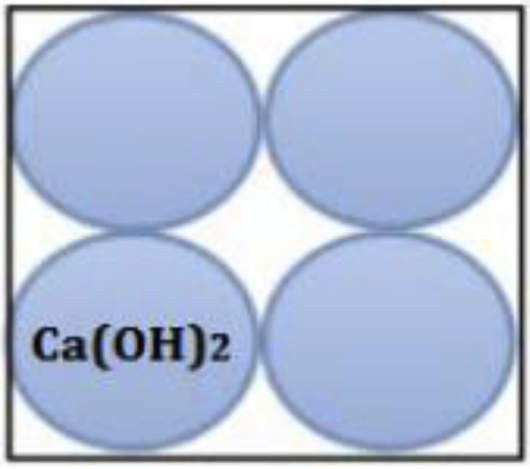

b) Free state

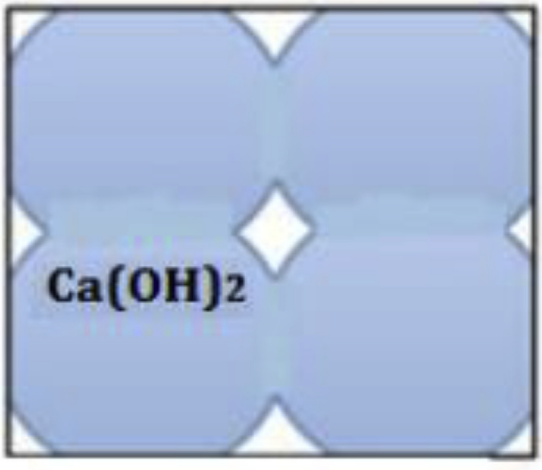

c) Restricted state

Fig. 5. Expanding model of static fracture agent.

$$\Delta V_{CaO} = \frac{33.07 - 16.74}{16.74} \times 100\% = 98\% \quad (5)$$

As $Ca(OH)_2$ is generated in the reaction of CaO and water, the solid volume expands by two times compared with its initial volume under free conditions. Simultaneously, the porosity also increases, while the simple volume variations do not produce swilling pressure. The slurry of fracturing agents without limitations expands and collapses into powders, while in cases where limitations exist in the surroundings, as $Ca(OH)_2$ expands and then extrudes, the porosity decreases and thus expand pressure emerges. In general, the tensile strength of brittle materials is much lower than compressive strength. In the improvement process, expand pressure takes place in the limited space in the surroundings. When it surpasses the ultimate bearing capacity of the space, the structure of the limited space is destroyed. The expansion model of chemical demolition agents is shown in Fig. 5.

4. Conclusions

This paper employed an orthogonal experiment to study the fracturing effects of a demolition agent with different proportions of various components and finally an optimum ratio was obtained. The primary components of the demolition agent consist of expansion source, water-reducer, retarder and cement, for which CaO, naphthalene-based water reducer, sodium gluconate and silicate cement were employed. The optimum proportion of CaO, naphthalene-based water reducer, sodium gluconate and silicate cement was 90:3:5:7 according to experimental result. Afterwards, a demolition agent with the optimum ratio was prepared and XRD phase analysis was performed on the agents without water as well as those at 5, 10 and 15 h after the addition of water. Accordingly, the authors researched the microstructures and component variations of the demolition agent, and discussed the variations of expand pressure during the process while the demolition agent played its role. The increased speed of expand pressure changes from the initial generation to complete release, with a high speed in the early stage and a slower speed in the later stages.

Conflict of interest

None.

References

Aguado, M. B. D., & Nicieza, C. G. (2007). Control and prevention of gas outbursts in coal mines, Riosa-Olloniego coalfield, Spain. *International Journal of Coal Geology, 69*(4), 253–266.

An, F. H., Cheng, Y. P., Wang, L., & Li, W. (2013). A numerical model for outburst including the effect of adsorbed gas on coal deformation and mechanical properties. *Computers and Geotechnics, 54*, 222–231.

An, H., Wei, X. R., Wang, G. X., Massarotto, P., Wang, F. Y., Rudolph, V., et al. (2015). Modeling anisotropic permeability of coal and its effects on CO2 sequestration and enhanced coalbed methane recovery. *International Journal of Coal Geology, 152*(Part B), 15–24.

Fukui, H., & Nagaishi, T. (2001). Static demolition by calcium oxide (IV): Thermal decomposition of calcium carbonate. *Journal of the Japan Explosives Society, 62*(1), 39–47.

Gambatese, J. A. (2003). Controlled concrete demolition using expansive cracking agents. *Journal of Construction Engineering and Management, 129*(1), 98–104.

Gao, Y., Fu, G., & Nieto, A. (2016). A comparative study of gas explosion occurrences and causes in China and the United States. *International Journal of Mining, Reclamation and Environment, 30*(4), 269–278.

Germanovich, L. N., Astakhov, D. K., Mayerhofer, M. J., Shlyapobersky, J., & Ring, L. M. (1997). Hydraulic fracture with multiple segments I. Observations and model formulation. *International Journal of Rock Mechanics and Mining Sciences, 34*(3–4), 472.

Hinze, J., & Nelson, A. (1996). Enhancing performance of soundless chemical demolition agents. *Journal of Construction Engineering and Management, 122*(2), 193–195.

Jiang, B. Y., Lin, B. Q., Shi, S. L., Zhu, C. J., & Li, Z. W. (2011). Theoretical analysis on the attenuation characteristics of strong shock wave of gas explosion. *Procedia Engineering, 24*, 422–425.

Karacan, C.Ö., Ruiz, F. A., Cotè, M., & Phipps, S. (2011). Coal mine methane: A review of capture and utilization practices with benefits to mining safety and to greenhouse gas reduction. *International Journal of Coal Geology, 86*(2), 121–156.

Lin, B. Q., Jiang, B. Y., Zhu, C. J., Zhai, C., Liu, Q., & Ye, Q. (2013). Influence of initial spherical flame radius on the explosion-proof safety distance, the flameproof distance, and the propagation characteristics of gas deflagrations. *Research Journal of Chemistry and Environment, 17*, 143–150.

Lin, B., Yan, F., Zhu, C., Zhou, Y., Zou, Q., Guo, C., et al. (2015). Cross-borehole hydraulic slotting technique for preventing and controlling coal and gas outbursts during coal roadway excavation. *Journal of Natural Gas Science and Engineering, 26*, 518–525.

Natanzi, A. S., & Laefer, D. F. (2015). Using chemicals as demolition agents near historic structures. *Paper presented at the 9th international conference on structural analysis of historical constructions*. Mexico City, Mexico, 14–17 October, 2014.

Song, D., Liu, Z., Wang, E., Qiu, L., Gao, Q., & Xu, Z. (2015). Evaluation of coal seam hydraulic fracturing using the direct current method. *International Journal of Rock Mechanics and Mining Sciences, 78*, 230–239.

Tang, Y. (2015). Methane drainage optimization by roof-borehole based on physical simulation. *Arabian Journal of Geosciences, 8*(10), 7879–7886.

Toraño, J., Torno, S., Alvarez, E., & Riesgo, P. (2012). Application of outburst risk indices in the underground coal mines by sublevel caving. *International Journal of Rock Mechanics and Mining Sciences, 50*, 94–101.

Wang, L., Cheng, Y. P., Ge, C. G., Chen, J. X., Li, W., Zhou, H. X., et al. (2013). Safety technologies for the excavation of coal and gas outburst-prone coal seams in deep shafts. *International Journal of Rock Mechanics and Mining Sciences, 57*, 24–33.

Xue, Y., Gao, F., Gao, Y., Cheng, H., Liu, Y., Hou, P., et al. (2016). Quantitative evaluation of stress-relief and permeability-increasing effects of overlying coal seams for coal mine methane drainage in Wulan coal mine. *Journal of Natural Gas Science and Engineering, 32*, 122–137.

Xue, S., & Yuan, L. (2017). The use of coal cuttings from underground boreholes to determine gas content of coal with direct desorption method. *International Journal of Coal Geology, 174*, 1–7.

Yuan, L. (2011). Theories and techniques of coal bed methane control in China. *Journal of Rock Mechanics and Geotechnical Engineering, 3*(4), 343–351.

Yuan, L. (2016). Control of coal and gas outbursts in huainan mines in China: A review. *Journal of Rock Mechanics and Geotechnical Engineering, 8*(4), 559–567.

Zhu, W. C., Gai, D., Wei, C. H., & Li, S. G. (2016). High-pressure air blasting experiments on concrete and implications for enhanced coal gas drainage. *Journal of Natural Gas Science and Engineering, 36*(Part B), 1253–1263.